Facies
January 2010, Volume 56, Number 1, Pages 13-25
http://dx.doi.org/10.1007/s10347-009-0196-2

A latitudinal gradient of seasonal temperature variation recorded in oyster shells from the coastal waters of France and The Netherlands

Franck Lartaud[1, 4, *], Laurent Emmanuel[1], Marc de Rafelis[1], Michel Ropert[2], Nathalie Labourdette[1], Christopher A. Richardson[3] and Maurice Renard[1]

[1] UPMC Paris 06, UMR 7193, ISTeP-Lab. Biominéralisations et Environnements sédimentaires, Case postale 116, 4 place Jussieu, 75252 Paris Cedex 05, France
[2] Laboratoire Environnement Ressource de Normandie (LERN), IFREMER, BP 32, Avenue du Général de Gaulle, 14520 Port-en-Bessin, France
[3] School of Ocean Sciences, College of Natural Sciences, Bangor University, Menai Bridge, Anglesey, LL59 5AB, UK
[4] Present address: IUEM-UBO, UMR CNRS 6539, Lab. Sciences de l'Environnement Marin (LEMAR), Technopôle Brest-Iroise, Place N. Copernic, 29280 Plouzané, France

*: Corresponding author : Lartaud F., email address : franck.lartaud@univ-brest.fr

Abstract:

Cathodoluminescence (CL) microscopy of the foliated calcite shell hinge sections of live-collected oyster *Crassostrea gigas* collected at seven locations along a latitudinal gradient from the Netherlands in the North Sea to the Atlantic coast of France, revealed variations in luminescence that were attributable to seasonal variations in calcification of the hinge. Photomicrographs of hinge sections and luminescence profiles were analyzed to define a micro-sampling strategy that was adopted to drill the hinge samples to determine their isotopic composition. Reconstructed seasonal seawater temperatures determined from the stable oxygen isotope ($\delta^{18}O$) composition along growth profiles from 32 oyster shell hinges showed distinct seasonal isotopic cycles that were compared with in situ measured seawater temperatures and salinities at each location. Comparison of the amplitude of the ($\delta^{18}O$) signal and the annual maximum and minimum seawater temperatures demonstrated that *C. gigas* shells from several locations provided a reliable record of seasonal seawater temperature variation. The exception to this was oysters from the Netherlands and northern France where winter growth rates at low temperatures were slow so that insufficient shell was deposited to allow adequate spatial resolution of sampling and this resulted in time-averaging of the reconstructed seawater temperatures and an overestimation of winter seawater temperature. A potential variability in $\delta^{18}O_w$–salinity relationship at low salinities could also explain the high difference between measured and predicted seawater temperatures in Dutch areas. The finding that latitudinal differences in oyster hinge growth rates and/or changes in the $\delta^{18}O_w$–salinity relationship can result in bias of the seawater temperature deduced from the stable isotopic composition of the hinge should be taken into account when reconstructing latitudinal gradients in seawater temperature.

Keywords: Mollusk shells - *Crassostrea gigas* - Cathodoluminescence - Stable isotopes - Palaeotemperatures - Seasonality

Introduction

The stable isotopic ($\delta^{18}O$) composition of calcite in mollusc shells has been shown to be a reliable proxy for changes in seawater temperature and salinity (e.g. Epstein et al. 1953; Carter 1980; Schein et al. 1991; Surge et al. 2001). The geochemical composition of bivalve shells can provide information on the temporal changes of a range of environmental factors over both long- (multi-annual), mid- (seasonal) and short-term (lunar and tidal) time scales (e.g. Arthur et al. 1983; Richardson 2001; Schöne 2003). Although many authors have utilised bivalve shells to reconstruct the seasonal evolution of environmental conditions at specific locations (e.g. Killingley and Berger 1979; Kennedy et al. 2001; Mueller-Lupp et al. 2003; Dettman et al. 2004; Schöne et al. 2004), few studies, however, have investigated the isotopic composition of mollusc shells along latitudinal gradients (see Jones and Quitmyer 1996; Khim et al. 2000; Elliot et al. 2003; Schöne et al. 2003). Harrington (1989) has underlined the importance of understanding the effects of geographical position on environmental records in shells of the same species.

Oysters of the genus *Crassostrea* and *Ostrea* are well suited to stable isotopic studies owing to their ability to deposit their shell in isotopic equilibrium with seawater over a wide range of ecological settings, from coastal shelf seas to intertidal areas (Hong et al. 1995; Kirby et al. 1998; Surge et al. 2001). Moreover, oysters have a wide latitudinal and temporal distribution in geological time (Stenzel 1971). The understanding and interpretation of the incorporation of shell oxygen isotopes requires a temporal frame within the shell from which to develop a model of shell growth. Many mollusc shells contain periodically deposited internal growth lines, checks and bands (Richardson 2001; Higuera-Ruiz et al. 2009; Wisshak et al. 2009) or external morphological growth rings and striae that can be used as chronological markers in or on the shell (e.g. Lawrence 1988; Kirby et al. 1998). However, these kinds of periodic structures are not always readily apparent or suitably preserved in all oyster species (Rhoads and Lutz 1980; Lartaud et al. 2006), and even when growth checks are present they do not always provide reliable annual records of shell growth (Surge et al. 2001).

Cathodoluminescence (CL) can provide an alternative approach for identifying growth increments within biogenic carbonate shells that are not normally visible using conventional microscopy (Barbin et al. 1991; Barbin 2000). The bombardment of biogenic carbonates with a cathode ray leads to the emission of photons by manganese ions (Mn^{2+}) resulting in luminescence of the ions within the shell matrix. Experimentally marking oyster shells with $MnCl_2$ produces an internal fluorescent line that can be detected in the shell under CL

(Langlet et al. 2006; Lartaud 2007). These induced fluorescent lines have been used to mark the beginning of growth in oyster shells to which all subsequent growth can be related and have been used to investigate the formation of microgrowth increments in the shell. Using the technique seasonal, spring-neap lunar and tidal patterns of growth increments have been observed in the hinge region of oyster *Crassostrea gigas*, shells from lagoonal environments e.g. Thau pond, France (Langlet 2002; Langlet et al. 2006) and from European Atlantic coasts (Lartaud 2007). These tidally deposited microgrowth lines have chronological significance and are-visible in CL and can be used to define the sample positions for drilling the calcite samples for isotope analysis.

In this paper we investigate the seasonal relationship between the stable isotope composition of oyster shell calcite and environmental conditions (seawater temperature and salinity). We use seasonal variations in luminescence in hinge sections and the tidal microgrowth increments to define the patterns of seasonal growth in the hinge region. We investigate whether the isotopic composition of the shells can be used reliably to reconstruct seasonal seawater temperatures in oysters collected at two locations in the Netherlands in the North Sea and at five locations along the French coastline.

Material and methods

Oysters *Crassostrea gigas,* were collected at seven locations along a transect from the Dutch North Sea to the north and north west Atlantic coastlines of France between latitude 53°N, north of the Netherlands, to 44°N in Arcachon basin, France (Fig. 1). Sampling of oysters occurred in two wave-sheltered Dutch sites (sites 1 and 2, Texel and Yerseke respectively) and at five coastal commercial French oyster farms (site 3, Baie des Veys (exposed) in the English Channel; site 4, Fort-Espagnol (wave-sheltered) in Brittany; site 5, Marennes-Oléron in Charente-Maritime (wave-sheltered); sites 6 and 7 Tès (wave-sheltered) and Ferret (exposed) respectively in Arcachon Basin). All of the locations are influenced by semi-diurnal tidal regimes. Daily measurements of seawater temperature and salinity at the oyster farms were provided by IFREMER (Institut Français de Recherche et d'Exploitation de la Mer) and in the Netherlands the Texel data were provided by the NIOZ (Royal Netherlands Institute for Sea Reseach, H. Van Aken, unpublished data, 2004). Only mean monthly records were available for Yerseke from the Dutch Center of Hydrology and Meteorology database (http://hmcz.nl).

In France, oyster *Crassostrea gigas* (Thunberg, 1793) spat, (size ~20 mm umbo-margin axis), were sourced from the IFREMER hatchery at La Tremblade, (Charente-Maritime) and transplanted until they were six months old into nursery tanks at Bouin (Vendée, Fig. 1). In these tanks the spat were fed daily for two weeks

with a diet of micro-algae (*Skeletonema costatum*) that had been cultured in seawater enriched with manganese (see Pirastru 1994; Hussenot and Buchet 1998) in order to internally mark their shells with a manganese spike that could be later identified with CL. These spats were then transplanted onto oyster tables at two locations (sites 3 and 4), Baie des Veys and Fort-Espagnol respectively. Oyster spat destined for transplantation at Marennes-Oléron (site 5) were transferred from nursery tanks at Bouin (Fig. 1) and held in an oyster pond for ~6 months (September 2001 to March 2002) before relaying onto oyster tables. Approximately 24-30 months after the oysters were relayed onto the oyster tables in February 2001 (site 5) and in March 2002 (sites 3 and 4) a sample of ~20 oysters were collected (see table 1). Oysters that had settled naturally during July 2001 in Arcachon basin were transplanted onto oyster tables in the Morbihan (France) during 12 months before located at sites 6 and 7, Tès and Ferret respectively and ongrown until they were collected in March 2004. The Netherlands oysters (40-50 mm and of unknown settlement date) were collected from natural wild recruited populations in October 2003. The growing conditions experienced by the oysters from the different regions are shown in Table 1.

Immediately upon collection the oysters were carefully opened in the field by cutting through the adductor muscle avoiding any damage to the hinge area and the flesh scrapped and removed from the inner surface of the shell valves to avoid any post-mortem carbonate dissolution following the oysters' aerial emersion. Upon return to the laboratory the shells were placed in a 6% solution of Hydrogen peroxide (H_2O_2) for 6 hours to remove any epibiota from the outer shell surfaces, washed in 0.15N Nitric acid for 20 minutes to dissolve any carbonate based superficial contamination and rinsed in demineralised water (5 mins.) The dry left shell valve of each oyster was cut along the maximum growth axis through the middle of the hinge region to the ventral shell margin (see Fig. 2).

The position of the annual growth lines and finer tidally deposited growth increments were determined from shell cross sections viewed under cathodoluminescence (see Langlet 2002; Langlet et al. 2006; Lartaud 2006 for methodologies). Cold cathode (Cathodyne-OPEA, 15-20 kV and 200 to 300 $\mu A.mm^{-2}$ under a pressure of 0.05 Torr) observations were made on the foliated calcite of the hinge section (see Fig. 3), because this area contains an ontogenetic record of both the oysters' hinge growth and the environmental conditions experienced throughout their life (Stenzel 1963; Carriker and Palmer 1979; Richardson et al. 1993; Kirby et al. 1998). Following the methodologies of Langlet et al. (2006) and Lartaud et al. (2006), CL-intensity variations across the hinge sections were analysed using the software Image J–1.33 (http://rsbweb.nih.gov/ij/) to determine

134 microscopic changes in CL that would reveal the patterns of incremental growth lines in the hinges of the oyster
135 shells. In this way, given the known date of death of the oyster shells and date of induction of a luminescent line
136 following laboratory exposure to manganese enriched algae, it was possible to assign a date to each of the tidal
137 increments and thus provide a chronology to the hinge growth which assisted in determining a
138 sclerochronological profile along the hinge that could be sampled for stable isotopes (see Fig. 3).

139 Samples of shell calcium carbonate for $\delta^{18}O$ and $\delta^{13}C$ analysis were drilled out, to a depth of ~ 0.1 mm,
140 from along each identified growth line in the foliated layers of the hinge region using a 0.5 mm diameter drill.
141 The number of drilled samples varied depending on the distance between each annual growth line. Collected
142 powders were acidified in 100% H_3PO_4 at 50°C under vacuum. The CO_2 produced was collected and analysed
143 using a mass spectrometer (VG Micromass 602). Isotopic data are reported in conventional delta (δ) notation
144 relative to the Vienna Pee Dee Belemnite (VPDB). The standard used for the analyses was an internal standard
145 calibrated on the NBS-19. Standard deviation for $\delta^{18}O$ and $\delta^{13}C$ is ±0.10‰.

146 Since salinity and $\delta^{18}O_{water}$ (‰ VSMOW) are known to be related, the measured seasonal average salinity
147 at each location was converted into $\delta^{18}O_{water}$ values using salinity/$\delta^{18}O_{water}$ relationships. Oxygen isotope data
148 from different coastal waters are affected by different estuarine river influx and evaporation rates in different
149 geographical areas (Schmidt 1999), therefore published $\delta^{18}O_{water}$–salinity equations specific to each oyster
150 location were applied to estimate the $\delta^{18}O_{water}$ values from the salinity data. For Texel (site 1), the equation of
151 Harwood et al. (2008) ($\delta^{18}O_{water}$=0.274xSalinity−9.3; R^2=0.89; N=247), for Yerseke (site 2), the equation of
152 Gillikin (2005) ($\delta^{18}O_{water}$=0.20xSalinity−6.31; R^2= 0.97; N=63) and for the French locations (site 3 to 7) the
153 equation of Lartaud (2007) established at different locations from the English Channel and the Atlantic coasts of
154 France ($\delta^{18}O_{water}$=0.22xSalinity−7.30; R^2=0.73; N=62) were used to convert the salinity data to $\delta^{18}O_{water}$. Shell
155 $\delta^{18}O$ data (‰VPDB) were then converted to seawater temperatures using the paleotemperature equation of
156 Anderson and Arthur (1983) derived from molluscan shells, where
157 $Temperature_{seawater}(°C)=16-4.14(\delta^{18}O_{shell}-\delta^{18}O_{water})+0.13\ (\delta^{18}O_{shell}-\delta^{18}O_{water})^2$. Because data set was small at
158 some locations, comparison between predicted and measured ST have been tested using the non-parametric
159 Mann-Whitney U test.
160
161 **Results**
162

163 The measured seasonal seawater temperature and salinities at each of the seven locations are shown in
164 Figure 4 and demonstrate a latitudinal gradient across the Dutch and French Locations. The maximum mean
165 annual seawater temperatures were 11.5°C and 12.8°C for the Netherlands and northern French locations
166 respectively, whereas the mean seawater temperatures in south west France were slightly higher at around
167 13.5°C. The northern French location, Fort-Espagnol (Brittany), showed a greater mean annual seawater
168 temperature of 16.8°C. The amplitude of the seasonal changes was variable from one site to another. The Dutch
169 sites from the shallow North Sea showed the greatest annual seawater temperature fluctuations; a difference of
170 24°C was recorded at Yerseke and 23°C at Texel. By contrast, oysters from Baie des Veys and Marenne-Oléron
171 showed a reduced seasonal contrast (between 15°C and 14°C). Mean salinities were lower at the Dutch locations
172 (27.8 PSU at Texel and 30.7 PSU at Yerseke) than at the French locations where the annual-mean salinities were
173 close to or >32 PSU The protected environments at Tes (in Arcachon Basin) and Texel sites (in the North Sea)
174 revealed the greater salinity ranges ~15 PSU whilst the more wave-exposed areas (Baie des Veys and Yerseke)
175 had the lowest variations (<5 PSU).

176 Profiles of $\delta^{18}O_{shell}$ and $\delta^{13}C_{shell}$ of the hinge regions are plotted as function of shell height in Figure 5.
177 $\delta^{18}O_{shell}$ of all of the oysters sampled from the seven locations show seasonal variations (Fig. 5 and Table 2).
178 Except for the shells from the Netherlands locations which have highly negative mean values (−1.4±0.6‰ for
179 Texel and −1.3±0.3‰ for Yerseke), the mean $\delta^{18}O_{shell}$ along the latitudinal gradient ranged between
180 −0.2±0.4‰ (Tes, Arcachon Basin) to 0.3±0.2‰ (Marennes-Oléron). Isotopic values for the shell part
181 corresponding to the nursery at Bouin (France) are slightly lower (−0.4±0.2‰). The maximum annual $\delta^{18}O_{shell}$
182 variations were observed at Baie des Veys and Tes (close to 2.0‰) whereas minimum variations were observed
183 in hinges of oysters from Yerseke (0.5‰) and Marennes-Oléron (0.9‰).

184 Conversion of the $\delta^{18}O_{shell}$ values into seawater temperature (ST) using the paleotemperature equation
185 produced a range of maximum and minimum ST's (Fig. 6 and Fig. 7). For example the hinge region of the shells
186 recorded ST maxima of 23.3°C at location 4 (Fort-Espagnol), 22.7 at location 2 (Yerseke) and 22.5°C at location
187 1 (Texel, see table 2), whilst minimum ST of 5.9°C were recorded in shells from location 5 (Marennes-Oléron,
188 France). The largest annual range in ST was observed at Tès (location 6) and at Fort-Espagnol (location 4), with
189 a range of 13.1°C and 11.2°C respectively. The lowest seasonal range (3.4°C) appeared in hinges of shells from
190 location 2 at Yerseke, in the Netherlands. The lowest mean annual ST was recorded in oysters from location 5 at
191 Marennes-Oléron (12.3±2.2°C) whereas shells from location 2 (Yerseke, the Netherlands) and to a lesser extent

192 from location 4 (Fort-Espagnol, France) showed the highest mean annual ST's (20.5±1.6°C and 16.4±1.0°C
193 respectively, see Figure 7). Only small differences were apparent in the average annual reconstructed ST
194 between oysters of the same age from the same site (Table 2). The average reconstructed summer ST from the
195 oyster hinges was not significantly different from the measured ST (Mann-Whitney test, $p<0.05$; Table 3) at all
196 locations, except Yerseke ($z=-2.698$, $p=0.003$; Table 3). By contrast the average predicted winter ST's were
197 significantly lower than the measured winter ST's in oysters from the northern locations (Texel and Yerseke in
198 the Netherlands, Baie-des-Veys in France; Table 3) and in Marennes-Oléron ($z=-2.252$, $p=0.012$), but not
199 significantly different at the other French locations.
200 $\delta^{13}C_{shell}$ do not show clear seasonal variations. Isotopic values are higher during summer in Yerseke,
201 Baie des Veys, Fort-espagnol, Marennes-Oléron and Ferret, but not in Texel and Tès (Figure 5). The average
202 $\delta^{13}C_{shell}$ values range from −1.9±0.2‰ (Yerseke) to −0.2±0.2‰ (Ferret, Arcachon Basin). The Dutch locations
203 and shell part corresponding to nursery at Bouin records the lower values (always lower than −1.4±0.2‰)
204 whereas French sites have mean values up to −0.7±0.1‰ (Table 2).
205
206 **Discussion**
207
208 The accuracy of the seawater temperature (ST) estimated from the $\delta^{18}O_{shell}$ together with low intra-
209 specific variability in the ST estimated from different oyster shell hinges demonstrates that considerable
210 confidence can be attached to the ST's from the foliated calcite shell of *Crassostrea gigas*. Mean annual ST's
211 determined from the $\delta^{18}O_{shell}$ compared favourably with *in situ* measurements of the mean annual ST range
212 across their studied latitudinal range. These results are in accordance with the works of Hong et al. (1995), Kirby
213 et al. (1998) and Surge et al. (2001) who demonstrated that oxygen isotopes are incorporated into oyster shells
214 close to isotopic equilibrium with seawater and without intra-specific fractionation. The observed almost exact
215 correspondence between the maximum estimated ST from the $\delta^{18}O_{shell}$ in oyster hinges, except those from
216 location 2 at Yerseke, and the maximum recorded measured summer *in situ* ST's strongly supports this.
217 By contrast the oyster shell hinges showed considerable variation in their ability to record the minimum
218 winter ST's. Shells from all the French locations except station 6 (Tès), where there was exact correspondence
219 between the estimated ST's from the $\delta^{18}O_{shell}$ and the *in situ* ST, recorded temperatures between 1 and 3°C
220 higher than the mean winter measured ST (Table 3). This disparity between the shell recorded winter minimum

221 ST and the measured ST was even greater in oyster hinges from the shallow boreal water locations in the North
222 Sea where a difference >5°C was apparent.

223 The lack of calcification in the American oyster *Crassostrea virginica* due to a skeletal growth break
224 during the coldest periods of the year (Loosanoff and Nomejko 1949; Galstoff 1964) may offer an explanation
225 for the difference between the predicted and observed ST's in this study. Quayle (1988) and Kirby et al. (1998),
226 for example, noted that shell deposition ceased in the shells of *C. gigas* from British Columbia, Canada, at
227 temperatures <10°C and Langlet et al. (2006) found that daily shell growth rates in oysters decreased from 30 to
228 10 µm between the summer and winter. Cessation in shell growth will introduce a gap in the isotopic values
229 during the winter period. A reduction in calcification rate during winter in *C.gigas* was observed to cause a
230 decrease in temporal resolution of the analytical sampling (Hong et al. 1995) and this probably resulted in time
231 averaging of the $\delta^{18}O_{shell}$ during the winter period. The resultant effect would be a mixing of winter and mid-
232 season $\delta^{18}O_{shell}$ in the drilled samples and would produce lower isotopic values (i.e. higher estimated winter
233 ST's) during the winter period than might have been expected (Harrington 1989; Goodwin et al. 2003).
234 However, our results suggest that seawater temperatures below 10°C can be clearly recorded in the shell
235 carbonate (i.e. ST records <8°C in Marennes-Oléron shells).

236 None of the Dutch oysters from Texel and Yerseke showed a good correlation between the $\delta^{18}O_{shell}$
237 predicted values and the observed ST's during the winter, when ST's were minimal, and during the summer the
238 oyster shells from Yerseke over-estimated the measured *in situ* ST's. Oysters from the more southern French
239 locations continued to grow, albeit slowly during the winter and this made it easier to drill discrete carbonate
240 samples and reconstruct the colder winter ST's in these regions than in the Northern Dutch sites. Dutch locations
241 where the growth experiments were conducted were exposed to salinity fluctuations as a result of anthropogenic
242 pressure causing large releases of freshwater during polder flooding, which cannot be recorded with monthly
243 measurements in Yerseke (see Material and methods). The decrease in salinity and high input of terrestrial
244 organic matter bring about both $\delta^{18}O_{shell}$ and $\delta^{13}C_{shell}$ reduction (Tivollier and Létolle 1968; Surge et al. 2001;
245 Gillikin et al. 2006). Isotopic measurements of seawater collected in the Scheldt estuary close to Yerseke by
246 Mook (1971), demonstrated that river inputs led to a −8.5‰ change in the isotope values which contributed to
247 the $\delta^{18}O_{water}$ value of seawater as −2‰ (SMOW). This estimation appears lower than our calculations using the
248 Gillikin (2005) equation, which used a $\delta^{18}O_{water}$ value from Yerseke of −0.23‰. The correction applied to the
249 $\delta^{18}O_{water}$ from Yerseke site led to a lower predicted ST (Figure 7). Even if these new predicted ST's are closer

to the measured *in situ* ST's, we cannot exclude the effect of slow winter shell growth rate fluctuations on the measured isotopic signals in the oyster shells. Any reconstruction of the seasonal amplitude of seawater temperatures should take this phenomenon into account.

Another explanations than a large decrease in shell growth rate for oysters from northern areas was given by Elliot et al. (2003). Using theoretical and measured $\delta^{18}O_w$ with latitude over the northern American continent, they show potential seasonal variability of the $\delta^{18}O_w$-salinity relationship. In their study, the low values of $\delta^{18}O_w$, corresponding to local river water inputs, where not monitored by the equation calibrated for most saline waters. However, strong difference between measured and predicted $\delta^{18}O_w$ appeared for salinities below 5 PSU in Elliot et al. (2003). No fall as much was observed in Dutch and French coastal waters but seasonal variations in the $\delta^{18}O_w$-salinity used in our works can be a field of investigation.

Summary

Cathodluminescence of polished radial sections of oyster *Crassostrea gigas* hinges demonstrated seasonal patterns of luminescence that were used to determine the oysters age and to establish a chronological scale along the shell hinges. The seasonal pattern of luminescence was used to define the positions for drilling of samples of shell carbonate for stable isotope analyses.

The $\delta^{18}O$ of oyster shells sampled from different coastal areas in the Netherlands and France allowed the latitudinal reconstruction of the annual seawater temperature range for specific locations along the French North Atlantic and Dutch North Sea. Hinges of *C. gigas* shells contain an ontogenetic record of the seawater temperature at which the shell was deposited and were reliably used to reconstruct the seasonal amplitude of seawater temperatures in oysters from locations along the French coastline. However, oysters from the Dutch North Sea and the north of France could not be used to determine the winter seawater minima because of (1) the slow growth rate of the hinge during winter lead to time averaging of isotopic records due to the mixing of winter and mid-season shell carbonate samples and (2) a potential variability in $\delta^{18}O_w$-salinity relationship at low salinities. Future reconstructions of the seasonal range of seawater temperatures from *C. gigas* shell hinges should take this into account.

Acknowledgements

280 The authors would like to thank Fabienne Rauflet, Edouard Bédier, Patrick Soletchnik, Philippe Geairon,
281 Danièle Maurer, Florence D'Amico and Marianne Alunno-Bruscia from IFREMER, as well as Joana Cardoso
282 from the NIOZ, for providing the oysters used in this investigation. This work could have been accomplished
283 without the hydrographic data from the IFREMER marine stations from Port-en-Bessin, Fort-Espagnol, La
284 Tremblade and Arcachon. This study was supported financially by the UPMC (Univ. Paris 06) via the Marc de
285 Rafelis BQR project High Frequency to Very High Frequency Recordings of Environmental Changes to Climate
286 by Biomineralizations ».
287
288 **References**
289
290 Anderson TF, Arthur MA (1983) Stable isotopes of oxygen and carbon and their application to sedimentologic
291 and paleoenvironmental problems. In: Arthur MA, Anderson TF, Kaplan IR, Veizer J, Land L (eds)
292 Stable Isotopes in Sedimentary Geology, vol. Society of Economic Paleontologists and Mineralogists,
293 Short Course, Dallas, pp 1-151
294 Arthur MA, Williams DF, Jones DS (1983) Seasonal temperature-salinity changes and thermocline in the mid-
295 Atlantic Bight as recorded by the isotopic composition of bivalves. Geology 11:655-659
296 Barbin V (2000) Cathodoluminescence of carbonate shells: biochemical vs diagenetic process. In: Pagel M,
297 Barbin V, Blanc P, Ohnenstetter D (eds) Cathodoluminescence in geosciences, vol. Springer Verlag,
298 Berlin, pp 303-329
299 Barbin V, Ramseyer K, Debenay JP, Schein E, Roux M, Decrouez D (1991) Cathodoluminescence of Recent
300 biogenic carbonates: an environmental and ontogenic fingerprint. Geol Mag 128(1):19-26
301 Carriker MR, Palmer RE (1979) A new mineralized layer in the hinge of the oyster. Science 206:691-693
302 Carter JG (1980) Selected mineralogical data for the Bivalvia. In: Rhoads DC, Lutz RA (eds) Skeletal growth of
303 aquatic organisms, vol. Plenum Press, New York, pp 627-643
304 Chauvaud L, Lorrain A, Dunbar RB, Paulet Y-M, Thouzeau G, Jean F, Guarini J-M, Mucciarone D (2005) Shell
305 of the Great Scallop *Pecten maximus* as a high frequency archive of paleoenvironmental change.
306 Geochem Geophys Geosyst 6:1-34
307 Dettman DL, Flessa KW, Roopnarine PD, Schöne BR, Goodwin DH (2004) The use of oxygen isotope variation
308 in shells of estuarine mollusks as a quantitative record of seasonal and annual Colorado River discharge.
309 Geochim. Cosmochim. Acta 68:1253-1263

310 Fröhlich K, Grabczak J, Rozanski K (1988) Deuterium and Oxygen-18 in the Baltic Sea. Chem Geol 72:77-83
311 Galstoff PS (1964) The American oyster, *Crassostrea virginica* Gmelin. US Fish Wild Serv Fish Bull 64:67-74
312 Gillikin DP (2005) Geochemistry of Marine Bivalve Shells: the potential for paleoenvironmental reconstruction.
313 PhD Thesis, Vrije Universiteit
314 Gillikin DP, Lorrain A, Bouillon S, Willenz P, Dehairs F (2006) Stable carbon isotopic composition of *Mytilus*
315 *edulis* shells: relation to metabolism, salinity, $\delta^{13}C$ DIC and phytoplancton. Organic Geochemistry 37:
316 1371-1382.
317 Goodwin DH, Schöne BR, Dettman DL (2003) Resolution and fidelity of oxygen isotopes as paleotemperature
318 proxies in bivalve mollusk shells: models and observations. Palaios 18:110-125
319 Harrington RT (1989) Aspects of growth deceleration in Bivalves: clues to understanding the seasonal $\delta^{18}O$ and
320 $\delta^{13}C$ record - A comment on Krantz et al. (1987). Palaeogeogr., Palaeoclimatol., Palaeoecol. 70:399-407
321 Harwood AJP, Dennis PF, Marca AD, Pilling GM, Milner RS (2008) The oxygen isotope composition of water
322 masses within the North Sea. Estuarine Coastal and Shelf Scie 78: 353-359
323 Higuera-Ruiz R, Elorza J (2009) Biometric, microstructural, and high-resolution trace element studies in
324 *Crassostrea gigas* of Cantabria (Bay of Biscay, Spain): Anthropogenic and seasonal influences. Estuarine
325 Coastal Shelf Sci 82:201-213
326 Hong W, Keppens E, Nielsen P, Van Riet A (1995) Oxygen and carbon isotope study of the Holocene oyster
327 reefs and paleoenvironmental reconstruction on the northwest coast of Bohai Bay, China. Mar. Geol.
328 124:289-302
329 Hussenot J, Buchet V (1998) Marais maritimes et aquaculture. Activités durables pour la préservation et
330 l'exploitation des zones humides littorales. In, vol. Quae, Versailles, p 279
331 Jones DS, Quitmyer IR (1996) Marking time with bivalve Shells: oxygen isotopes and season of annual
332 increment formation. Palaios 11:340-346
333 Kennedy H, Richardson CA, Duarte CM, Kennedy DP (2001) Oxygen and carbon isotopic profiles of the fan
334 mussel, *Pinna nobilis*, and reconstruction of sea surface temperatures in the Mediterranean. Mar Biol
335 139:1115-1124
336 Khim B-K, Woo KS, Je J-G (2000) Stable isotope profiles of bivalve shells: seasonal temperature variations,
337 latitudinal temperature gradients and biological carbon cycling along the east coast of Korea. Cont. Shelf
338 Res. 20:843-861

339 Killingley JS, Berger WH (1979) Stable isotopes in a mollusk shell: detection of upwelling events. Science
340 205(13):186-188
341 Kirby MX (2001) Differences in growth rate and environment between Tertiary and Quaternary *Crassostrea*
342 *oyster*. Paleobiology 27(1):84-103
343 Kirby MX, Soniat TM, Spero HJ (1998) Stable isotope sclerochronology of Pleistocene and Recent oyster shells
344 (*Crassostrea virginica*). Palaios 13:560-569
345 Langlet D (2002) Enregistrement haute fréquence des conditions environnementales par les tests de bivalves.
346 Application des techniques de marquage, cathodoluminescence, et chimie à l'huître *Crassostrea gigas* de
347 l'étang de Thau (Hérault, France). PhD Thesis Univ UPMC-Paris 06
348 Langlet D, Alunno-Bruscia M, Rafélis M, Renard M, Roux M, Schein E, Buestel D (2006) Experimental and
349 natural manganese-induced cathodoluminescence in the shell of the Japanese oyster *Crassostrea gigas*
350 (Thunberg, 1793) from Thau Lagoon (Hérault, France): ecological and environmental implications. Mar.
351 Ecol. Prog. Ser. 317:143-156
352 Lartaud F, Langlet D, de Rafelis M, Emmanuel L, Renard M (2006) Description of seasonal rythmicity in fossil
353 osyter shells *Crassostrea aginensis* Tournouer, 1914 (Aquitanian) and *Ostrea bellovacina* Lamarck, 1806
354 (Thanetian). Cathodoluminescence and sclerochronological approaches. Geobios 39:845-852
355 Lartaud F (2007) Les fluctuations haute fréquence de l'environnement au cours des temps géologiques. Mise au
356 point d'un modèle de référence actuel sur l'enregistrement des contrastes saisonniers dans l'Atlantique
357 nord. PhD Thesis Univ. UPMC-Paris 06
358 Lawrence DR (1988) Oysters as geoarcheologic objects. Geoarcheology 3:267-274
359 Loosanoff VL, Nomejko CA (1949) Growth of oysters, *O. virginica*, during different months. Biol Bull 97:82-94
360 Mook WG (1971) Paleotepemratures and chlorinities from stable carbon and oxygen isotopes in shell carbonate.
361 Palaeogeogr., Palaeoclimatol., Palaeoecol. 9:245-263
362 Mueller-Lupp T, Erlenkeuser H, Bauch HA (2003) Seasonal and interannual variability of Siberian river
363 discharge in the Laptev Sea inferred from stable isotopes in modern bivalves. Boreas 32:292-303
364 Pirastru L (1994) The Bay of Bourgneuf underground salt water: physicochemical characteristics, bioavailability
365 of phosphates and potential fertility for *Skeletonema costatum* (Grev.) Cleve. PhD Thesis Univ. Nantes
366 Quayle DB (1988) Pacific oyster culture in British Columbia. Can. Bull. Fish. Aquatic Sci. 218:241
367 Rhoads DC, Lutz RA (1980) Skeletal growth of aquatic organisms: biological records of environmental change,
368 Plenum Press, New York, p 750

Richardson CA, Collis SA, Ekaratne K, Dare P, Key D (1993) The age determination and growth rate of the European flat oyster, *Ostrea edulis*, in British waters determined from acetate peels of umbo growth lines. ICES J. Mar. Sci. 50:493-500

Richardson CA (2001) Molluscs as archive of environmental change. Oceanography and Marine Biology - An Annual Review 39:103-164

Schein E, Roux M, Barbin V, Chiesi F, Renard M, Rio M (1991) Enregistrement des paramètres écologiques par la coquille des bivalves: approche pluridisciplinaire. Bull. Soc. Geol. Fr. 162:687-698

Schmidt GA (1999) Forward modeling of carbonate proxy data from planktonic foraminifera using oxygen isotope tracers in a global ocean model. Paleoceanography 14:482-498

Schöne BR (2003) A "clam-ring" master-chronology constructed from a short-lived bivalve mollusc from the northern Gulf of California, USA. The Holocene 13:39-49

Schöne BR, Tanabe K, Dettman DL, Sato S (2003) Environmental controls on shell growth rates and $\delta^{18}O$ of the shallow-marine bivalve mollusk *Phacosoma japonicum* in Japan. Mar. Biol. 142:473-485

Schöne BR, Freyre Castro AD, Fiebig J, Houk SD, Oschmann W, Kröncke I (2004) Sea surface water temperatures over the period 1884-1983 reconstructed from oxygen isotope ratios of a bivalve mollusk shell (*Arctica islandica*, southern North Sea). Palaeogeogr., Palaeoclimatol., Palaeoecol. 212:215-232

Stenzel HB (1963) Aragonite and calcite as constituents of adult oyster shells. Science 142:232-233

Stenzel HB (1971) Oysters. In: Moore RC (ed) Treatise in Invertebrate Paleontology, Mollusca 6, Bivalvia., vol. Geological Society of America, University of Kansas, pp 271

Surge D, Lohmann KC, Dettman DL (2001) Controls on isotopic chemistry of the American oyster, *Crassostrea virginica*: implications for growth patterns. Palaeogeogr., Palaeoclimatol., Palaeoecol. 172:283-296

Tivollier J, Létolle R (1968) Résultat et interprétation d'analyses isotopiques de faunes malacologiques du Tertiaire parisien. Bureau de Recherches Géologiques et Minières, Memoires, Paris, pp 347-358.

Wisshak M, Lopez-Correa M, Gofas S, Salas C, Taviani M, Jakobsen J, Freiwald A (2009) Shell architecture, element composition, and stable isotope signature of the giant deep-sea oyster *Neopycnodonte zibrowii* sp. n. from the NE Atlantic. Deep Sea Research I 56:374-407

Legends to tables:

Table 1: Summary of the locations where *Crassostrea gigas* were collected from the Netherlands and France.

Table 2: Average and range of carbon isotope composition and predicted seawater temperatures determined from oxygen isotope ratios in replicate oyster *Crassostrea gigas* shell hinges from seven locations in the Netherlands and France.

Table 3: Comparison of the summer and winter predicted seawater temperatures calculated from the stable isotopic composition of the hinges of oyster, *Crassostrea gigas* shells and the measured seawater temperature range at seven different locations in the Netherlands and France. Significant difference between the predicted and measured seawater temperatures are shown * ($p<0.05$).

Legends to figures:

Figure 1: Map to show the seven locations in the Netherlands and France where the oyster *Crassostrea gigas,* shells were transplanted and collected. The Netherlands locations (1) Texel and (2) Yerseke and the French locations, (3) Baie des Veys, (4) Fort-Espagnol, (5) Marennes-Oléron, (6) Tès, and (7) Ferret are shown. The inset shows in detail the positions of sites 6 and 7 in Arcachon Bay. Nursery tanks were located at Bouin (Nur). B : Belgium ; D ; Netherlands ; DK : Germany ; F : France ; MO ; Morrocco ; NL ; Netherlands ; P : Portugal ; SP : Spain ; SW : Switzerland ; UK : United Kingdom.

Figure 2: Left shell valve of *Crassostrea gigas* showing the position of the hinge region and inset the appearance of a polished radial section of the foliated calcite hinge sectioned through its longest axis.

Figure 3: Upper figure composite photomicrograph of the hinge region of the oyster *Crassostrea gigas* (shell number PBr13, from Baie des Veys to illustrate the seasonal variation in cathodoluminescence along the transect A-A'. Middle figure, more luminescent areas are associated with the summer period of hinge growth whereas during winter deposition of the hinge a low level of luminescence occurs and lower figure allocation of periods of luminescence to calendar dates.

Figure 4: Comparison of the seasonal variation in seawater temperature (black line) and salinity (grey line) from the seven different study locations.

Figure 5: Seasonal changes in $\delta^{18}O$ (closed circles) and $\delta^{13}C$ (open circles) in *Crassostrea gigas* shells grown at the seven study locations. Note that the $\delta^{18}O$ axis has been inverted. The gray bands correspond to the nursery period at Bouin station. The number of each oyster analysed is in parenthesis. A: Texel (Te 3); B: Yerseke (Ye 1); C: Baie des Veys (PBr13); D: Fort-Espagnol (FEs 20); E: Marennes-Oléron (MO 17); F: Tès (TES 2); G: Ferret (FERT 6).

Figure 6: Comparison of the *in situ* measured (grey) and reconstructed (black) seawater temperatures for different *Crassostrea gigas* shells grown at seven locations along a latitudinal gradient from the Dutch North Sea to the French North-East Atlantic coasts. Each shell number is shown in parentheses. A: Texel (Te 3); B:

441 Yerseke (Ye 1); C: Baie des Veys (PBr13); D: Fort-Espagnol (FEs 20); E: Marennes-Oléron (MO 17); F: Tès
442 (TES 2); G: Ferret (FERT 6).
443
444 Figure 7: Comparison of the amplitude of the reconstructed seawater temperatures determined from stable
445 isotopes in shell carbonate (black). Winter minimum seawater temperatures (bottom black rectangles), summer
446 maximum (top black rectangles) and annual average temperatures (black circles) recorded in oyster shells along
447 the European North Atlantic and North Sea coasts. The amplitudes of the measured *in situ* seawater temperatures
448 are shown in grey, and those calculated from isotopic ratios of the shells are in black. Dotted black lines for
449 Dutch sites represent paleotemperature estimation using Mook's (1971) $\delta^{18}O_{water}$ measurements. F: France,
450 NL: Netherlands.
451

Figure 1

Click here to download high resolution image

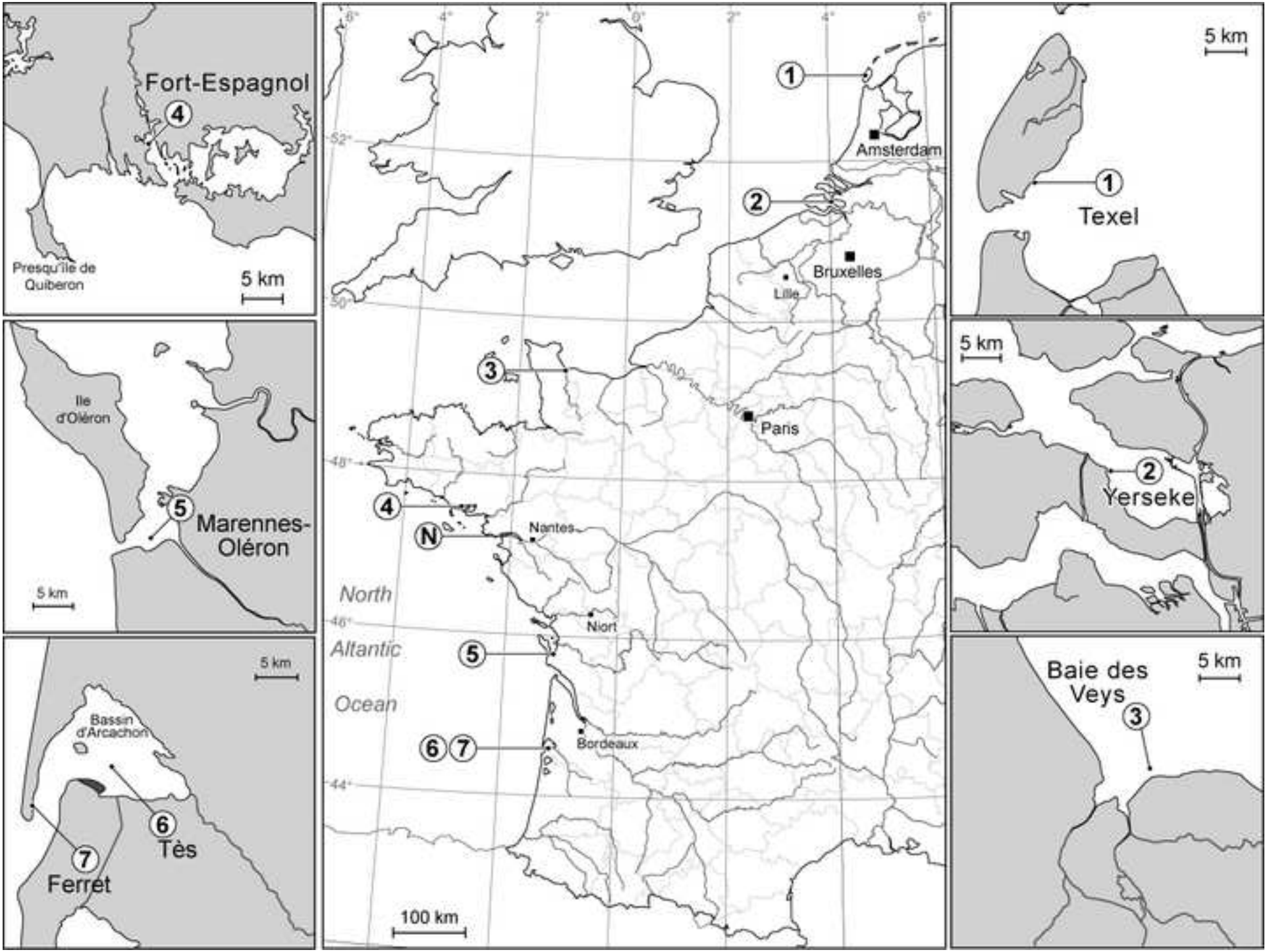

Figure 2

Click here to download high resolution image

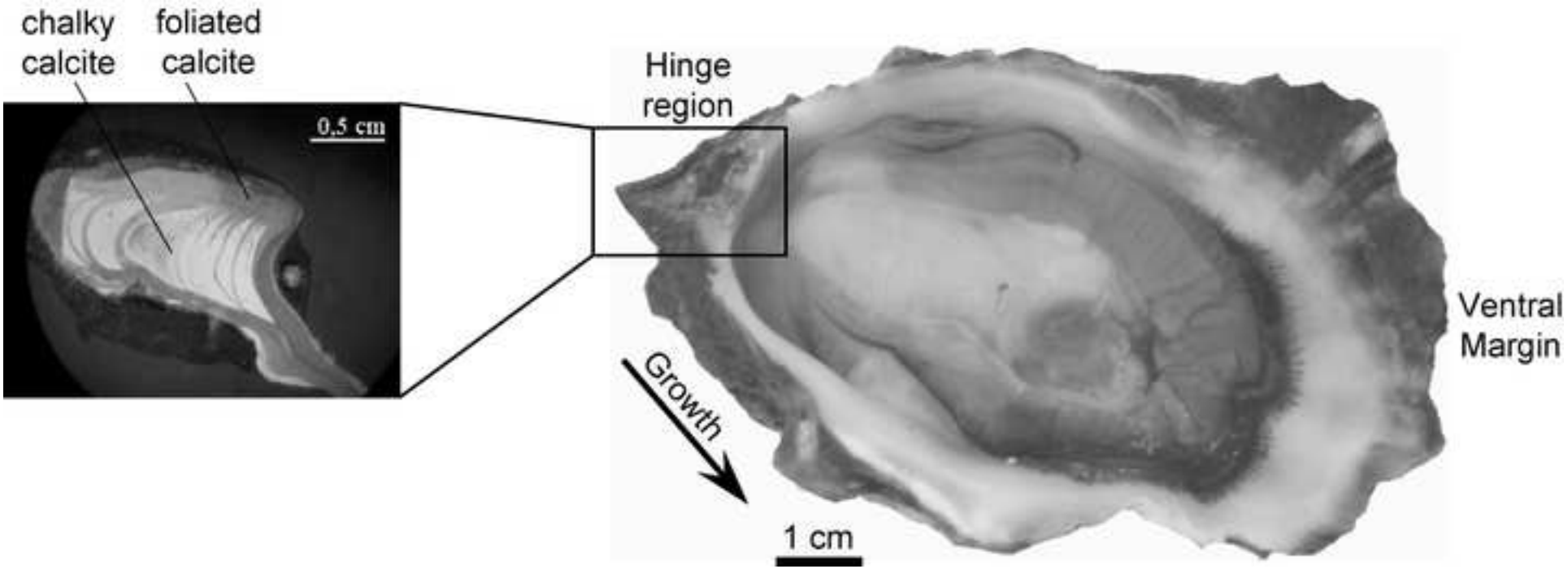

Figure 3

Click here to download high resolution image

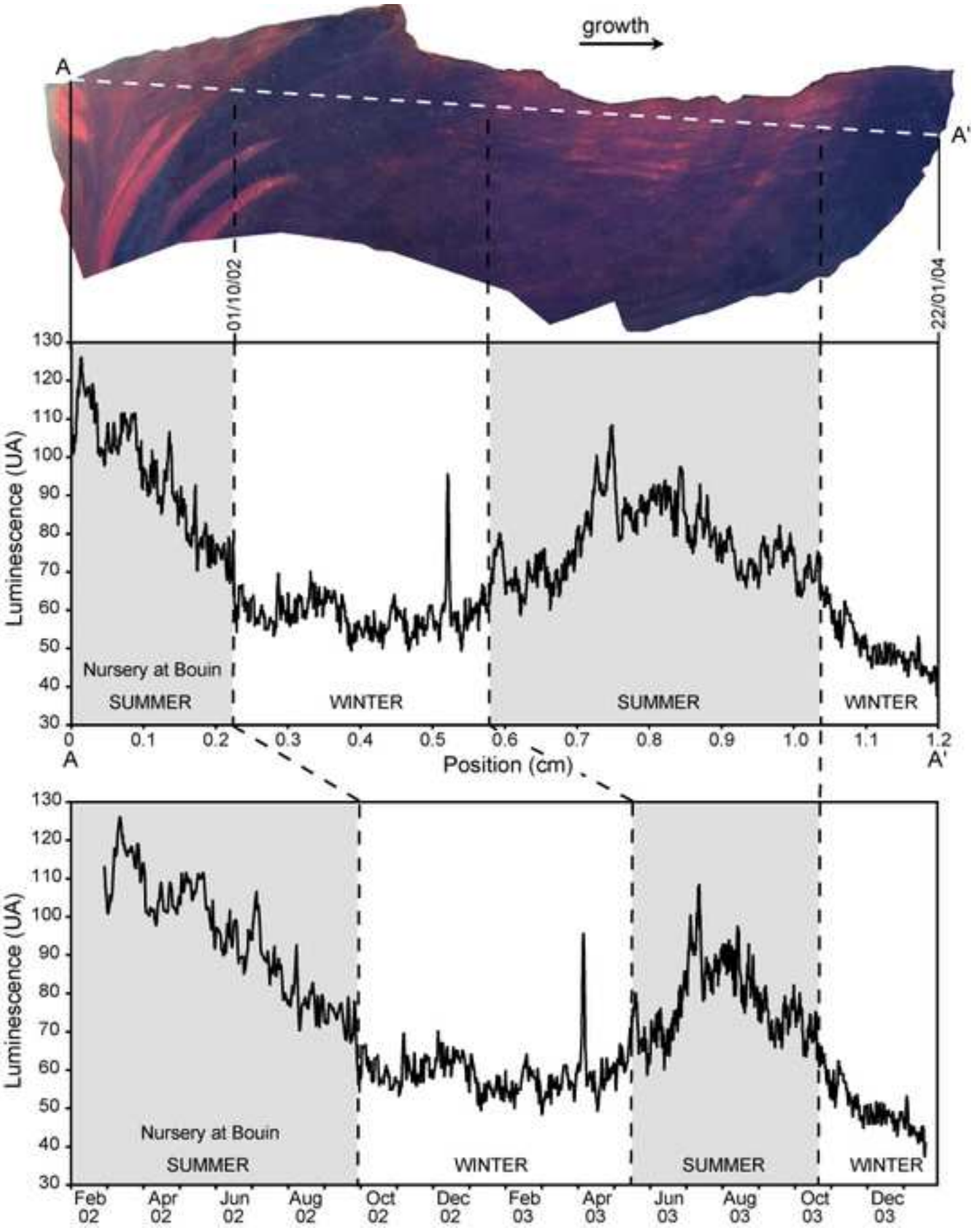

Figure 4

Click here to download high resolution image

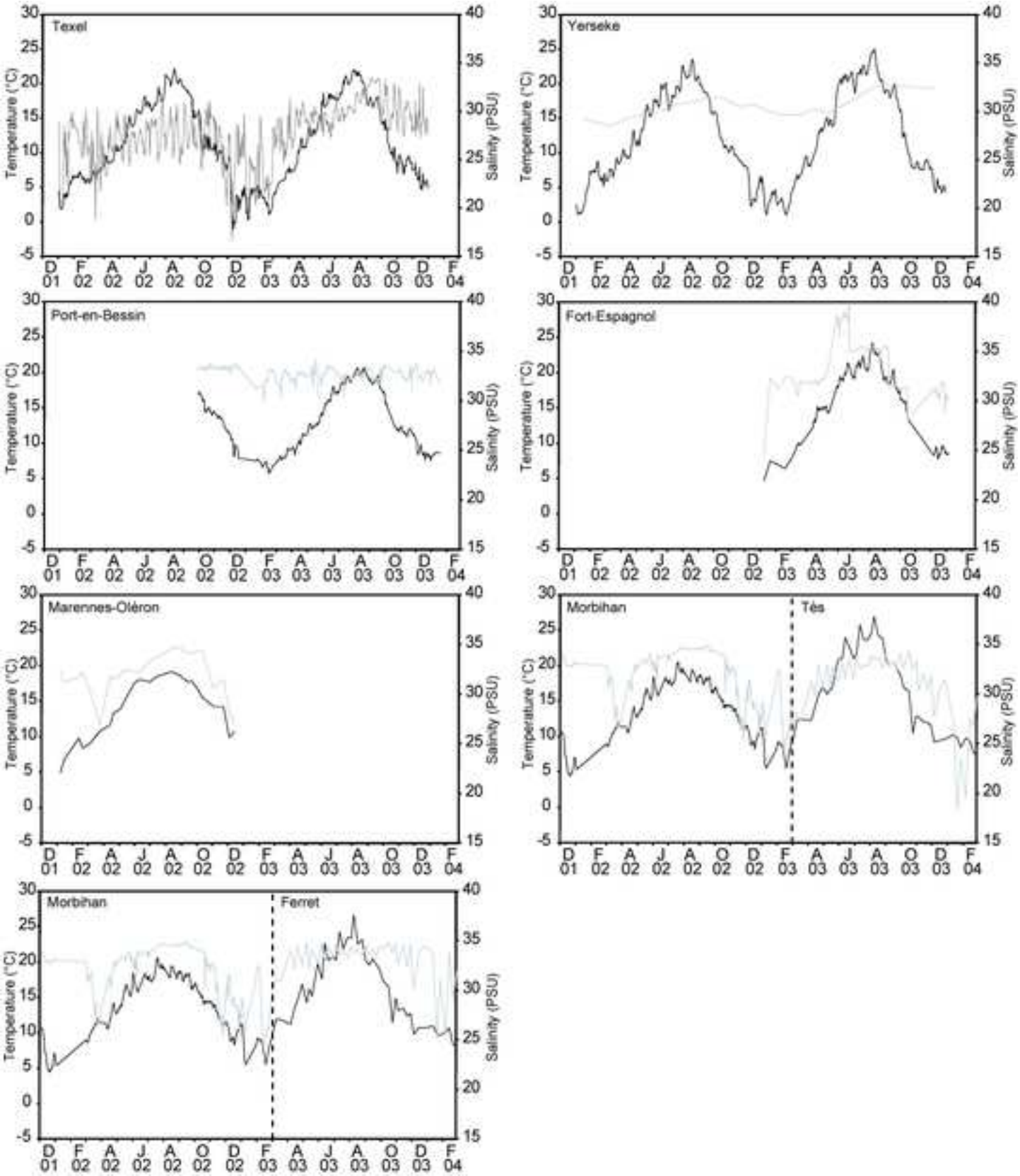

Figure 5

Click here to download high resolution image

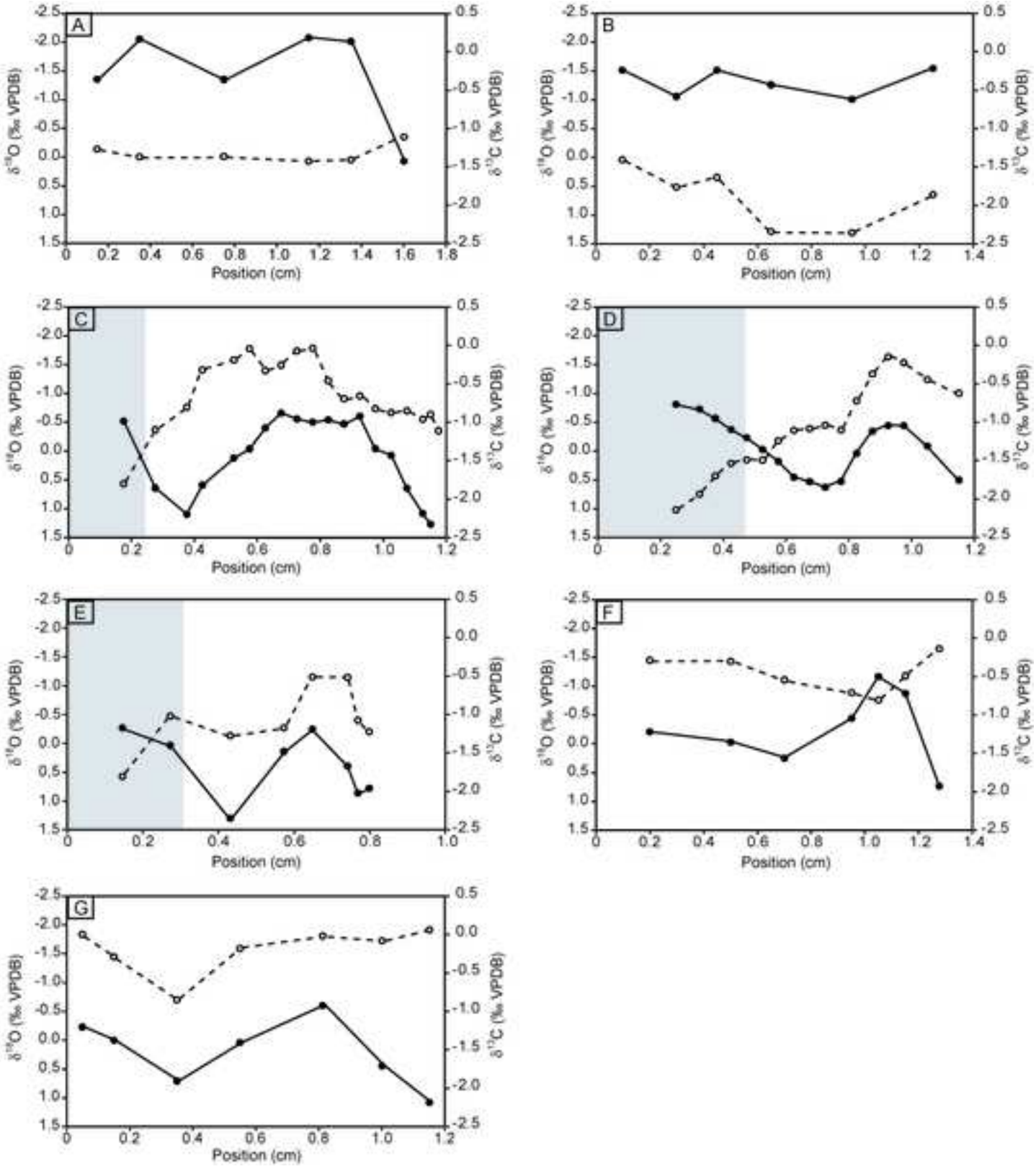

Figure 6

Click here to download high resolution image

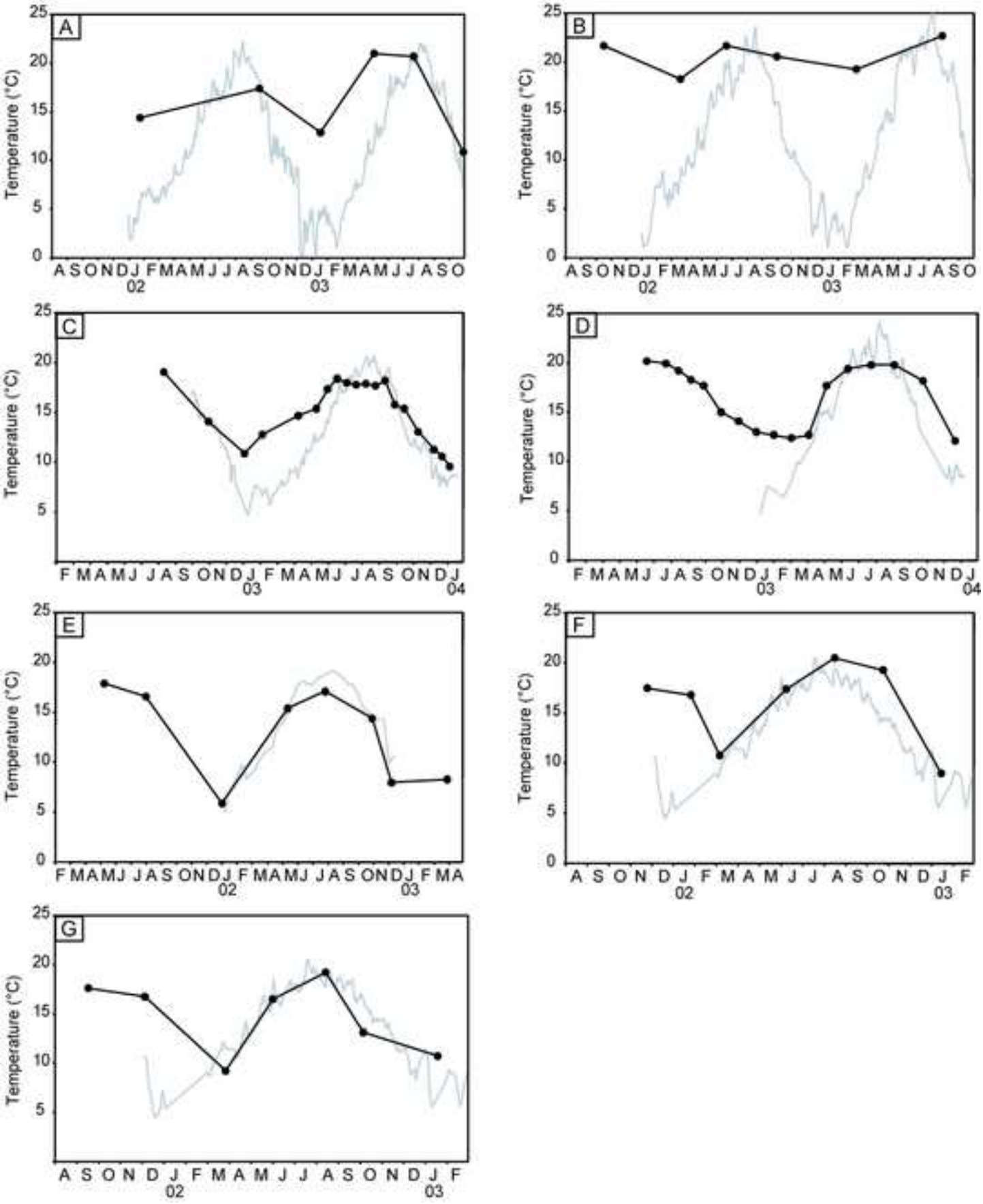

Figure 7

Click here to download high resolution image

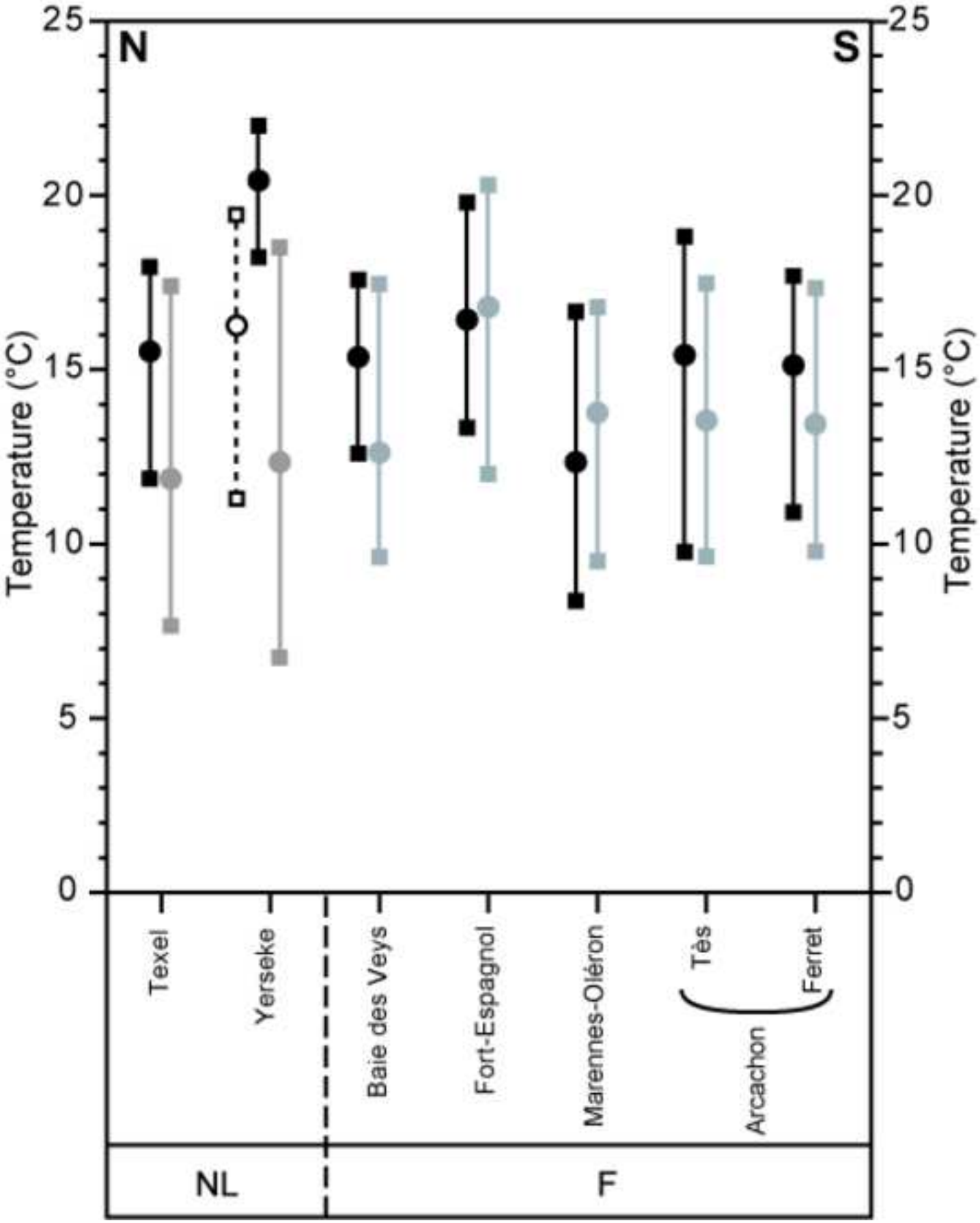

Table 1

Location		Protected (P) or exposed (E) location	No. of oysters analysed for stable oxygen isotopes	Natural (N) or hatchery spat (H)	Date of oyster spat settlement	Date of collection of oysters
Netherlands						
Texel	1	P	2	N	Unknown	October 2003
Yerseke	2	P	2	N	Unknown	October 2003
France						
Baie des Veys	3	E	7	H	March 2002	January 2004
Fort-Espagnol	4	P	6	H	March 2002	January 2004
Marennes-Olèron	5	P	4	H	February 2001	April 2003
Tès	6	P	2	N	July to August 2001	March 2004
Ferret	7	E	2	N	July to August 2001	March 2004

Table 2

Shell	Locality	Samples drilled per shell	Mean $\delta^{13}C$	min / max	Mean $\delta^{18}O$	min / max	Mean predicted T° (°C)	min / max
Te 1	Texel (the Netherlands)	4	-1.45	-1.83 / -0.89	-1.33	-2.48 / -0.69	14.4	10.6 / 19.4
Te 3	Texel (the Netherlands)	6	-1.33	-1.43 / -1.11	-1.47	-2.08 / 0.07	16.2	10.9 / 21.0
Ye 1	Yerseke (the Netherlands)	7	-1.89	-2.36 / -1.40	-1.32	-1.55 / -1.01	20.7	18.3 / 22.7
Ye 2	Yerseke (the Netherlands)	4	-1.81	-2.13 / -1.54	-1.16	-1.71 / -0.17	20.3	16.7 / 22.6
PBr 1	Baie des Veys (France)	16	-1.16	-1.57 / -0.76	0.05	-0.89 / 1.52	15.4	9.6 / 19.4
PBr 12	Baie des Veys (France)	13	-0.91	-1.26 / -0.39	0.29	-0.73 / 1.38	14.4	10.1 / 18.7
PBr 13	Baie des Veys (France)	17	-0.64	-1.80 / -0.03	0.13	-0.66 / 1.52	15.2	9.6 / 19.0
PBr 15	Baie des Veys (France)	8	-1.32	-1.73 / -1.02	-0.11	-1.14 / 0.99	16.0	11.3 / 20.5
PBs 3	Baie des Veys (France)	14	-1.04	-1.53 / -0.53	0.04	-0.81 / 1.25	15.4	10.6 / 19.1
PBs 16	Baie des Veys (France)	14	-0.58	-1.39 / 0.16	0.03	-0.83 / 1.11	15.4	11.2 / 19.2
PBs 21	Baie des Veys (France)	16	-1.11	-2.04 / -0.76	-0.75	-0.98 / 1.05	15.7	11.0 / 19.8
FEr 9	Fort-Espagnol (France)	7	-0.66	-1.51 / -0.10	-0.51	-1.24 / 0.14	18.7	14.0 / 23.3
FEr 15	Fort-Espagnol (France)	8	-0.38	-1.15 / 0.01	-0.01	-0.66 / 0.66	16.3	12.2 / 20.7
FEr 21	Fort-Espagnol (France)	6	-0.72	-1.21 / -0.45	0.20	-0.63 / 0.98	15.5	10.2 / 20.6
FEs 6	Fort-Espagnol (France)	10	-0.52	-1.27 / -0.09	0.09	-0.65 / 1.17	15.9	9.5 / 20.7
FEs 18	Fort-Espagnol (France)	8	-0.87	-1.37 / -0.31	-0.16	-0.84 / 0.34	17.0	12.7 / 21.5
FEs 20	Fort-Espagnol (France)	12	-0.80	-1.49 / -0.15	0.12	-0.45 / 0.63	15.6	12.1 / 20.2
MO 5	Marennes-Oléron (France)	7	-1.12	-1.76 / -0.44	0.03	-0.61 / 0.73	13.9	7.9 / 18.6
MO 6	Marennes-Oléron (France)	5	-1.20	-2.32 / -0.31	0.12	-0.37 / 0.76	12.4	7.8 / 17.5
MO 9	Marennes-Oléron (France)	5	-1.38	-2.28 / -0.68	0.16	-0.24 / 0.65	11.1	8.2 / 17.0
MO 17	Marennes-Oléron (France)	6	-0.96	-1.27 / -0.51	0.54	-0.25 / 1.30	11.5	5.9 / 17.1
TES 1	Tès - Arcachon (France)	6	-0.55	-0.71 / -0.34	-0.22	-1.46 / 0.79	14.7	8.7 / 21.8
TES 2	Tès - Arcachon (France)	7	-0.46	-0.80 / -0.13	-0.25	-1.17 / 0.73	15.9	9.0 / 20.5
FERT 5	Ferret - Arcachon (France)	6	-0.28	-0.58 / 0.00	0.05	-0.80 / 0.95	15.4	10.3 / 20.1
FERT 6	Ferret - Arcachon (France)	7	-0.19	-0.85 / 0.06	0.21	-0.60 / 1.08	14.7	9.2 / 19.2
PBr1	Bouin nursery (France)	2	-1.96		-0.75		20.0	
PBr 12	Bouin nursery (France)	1	-1.10		0.34		15.3	
PBr 13	Bouin nursery (France)	2	-1.45		0.06		16.6	
PBr 15	Bouin nursery (France)	1	-2.20		-0.26		17.8	
PBs 3	Bouin nursery (France)	3	-1.81		-0.73		19.9	
PBs 16	Bouin nursery (France)	2	-1.64		-0.18		17.5	
PBs 21	Bouin nursery (France)	1	-2.32		-0.56		19.1	
FEr 9	Bouin nursery (France)	2	-1.93		-0.43		18.6	
FEr 15	Bouin nursery (France)	1	-1.54		0.12		16.2	
FEr 21	Bouin nursery (France)	3	-1.97		-0.50		18.9	
FEs 6	Bouin nursery (France)	1	-1.93		-0.82		20.2	
FEs 18	Bouin nursery (France)	1	-2.05		-0.77		20.1	
FEs 20	Bouin nursery (France)	5	-1.76		-0.54		19.1	
MO 5	Bouin nursery (France)	2	-2.01		-0.42		18.6	
MO 6	Bouin nursery (France)	1	-1.77		-0.26		17.9	
MO 9	Bouin nursery (France)	1	-2.24		0.01		16.7	
MO 17	Bouin nursery (France)	2	-1.41		-0.12		17.3	

Table 3

Localities	Number of shells	Season	Predicted temperatures	Average sea water temperatures (summer: May to Oct) (winter: Oct to May)	Difference between predicted - measured temperatures	Mann-Whitney test	
Texel	2	summer	18.0±2.9	17.4±0.3	0.6	-0.972	
		winter	11.9±2.0	6.7±0.3	5.2	-2.577	*
Yerseke	2	summer	22.0±0.8	18.6±0.3	3.4	-2.698	*
		winter	18.2±2.7	6.8±0.3	11.4	-2.985	*
Baie des Veys	7	summer	17.6±0.4	17.5±0.4	0.5	-0.589	
		winter	12.6±0.5	9.6±0.3	3	-7.959	*
Fort-Espagnol	6	summer	19.8±0.6	20.3±0.3	0.5	1.842	
		winter	13.2±0.5	12.0±0.7	1.2	-0.475	
Marennes-Oléron	4	summer	16.7±1.0	16.8±1.1	0.1	0.507	
		winter	8.3±0.8	9.5±1.7	1.2	2.252	*
Tès	2	summer	18.8±1.4	17.4±0.4	1.4	-1.721	
		winter	9.8±1.1	9.7±0.3	0.1	-0.052	
Ferret	2	summer	17.7±1.2	17.3±0.3	0.4	-0.872	
		winter	10.9±1.8	9.8±0.3	1.9	-0.691	